Lithos 388–389 (2021) 106085

Contents lists available at ScienceDirect

Lithos

journal homepage: www.elsevier.com/locate/lithos

Research article

Trace elements in olivine: Proxies for petrogenesis, mineralization and discrimination of mafic-ultramafic rocks

Jing Wang [a,b,c,*], Ben-Xun Su [a,b,c,*], Paul T. Robinson [a], Yan Xiao [c,d], Yang Bai [a,b,c], Xia Liu [a,b,c], Patrick Asamoah Sakyi [e], Jie-Jun Jing [f], Chen Chen [g], Zi Liang [a], Zhi-An Bao [h]

[a] Key Laboratory of Mineral Resources, Institute of Geology and Geophysics, Chinese Academy of Sciences, Beijing 100029, China
[b] Innovation Academy for Earth Science, Chinese Academy of Sciences, Beijing 100029, China
[c] University of Chinese Academy of Sciences, Beijing 100049, China
[d] State Key Laboratory of Lithospheric Evolution, Institute of Geology and Geophysics, Chinese Academy of Sciences, Beijing 100029, China
[e] Department of Earth Science, University of Ghana, P.O. Box LG 58, Legon-Accra, Ghana
[f] Department of Earth Sciences, Faculty of Science, Vrije Universiteit Amsterdam, De Boelelaan 1085, 1081 HV Amsterdam, the Netherlands
[g] Key Laboratory of Mineralogy and Metallogeny, Guangzhou Institute of Geochemistry, Chinese Academy of Sciences, Guangzhou 510460, China
[h] State Key Laboratory of Continental Dynamics, Department of Geology, Northwest University, Xi'an 710069, China

ARTICLE INFO

Article history:
Received 12 September 2020
Received in revised form 23 February 2021
Accepted 25 February 2021
Available online 05 March 2021

Keywords:
Olivine
Trace elements
Mantle xenolith
Ophiolite
Layered intrusion
Alaskan-type intrusion

ABSTRACT

Olivine is a ubiquitous mineral in mafic-ultramafic rocks and has been widely used as a mineral marker in various geological processes. However, its development of trace elements is limited. Here we present newly-obtained trace element data ^{7}Li, ^{27}Al, ^{29}Si, ^{31}P, ^{43}Ca, ^{45}Sc, ^{49}Ti, ^{51}V, ^{53}Cr, ^{55}Mn, ^{59}Co, ^{60}Ni, and ^{66}Zn of olivine in typical mantle xenoliths, mantle peridotites in ophiolites, and plutonic rocks from layered and Alaskan-type intrusions to develop trace element proxies for the petrogenesis, mineralization and discrimination of various mafic-ultramafic rocks. Residual olivine grains in mantle xenoliths and ophiolitic peridotites, which represent residues of mantle melting, have higher Ni/Co (>20) and Ni/Mn (>2) ratios than magmatic olivine (Ni/Co < 20, Ni/Mn < 2), which are consistent with the compatibilities of these elements during partial melting and magma differentiation. Lower Ni content, and lower Ni/Co and Ni/Mn ratios at a given Fo content can distinguish olivine in Alaskan-type intrusions from layered intrusions, reflecting the nature of their mantle sources. The V and Sc contents and V/Sc ratios in olivine can distinguish mantle xenoliths (V > 2 ppm, V/Sc > 0.5) from ophiolitic peridotites (V < 2 ppm, V/Sc < 0.5), indicating a more reduced state of continental lithospheric mantle compared to the oceanic lithospheric mantle. As a consequence, the four occurrences of mafic-ultramafic rocks can be distinguished by olivine with (Sc × 10)-(Ti × 2)-Zn and V/Sc-(Co/Ni × 2)-(Zn/Mn × 5) ternary diagrams. In addition, Li, Ti and P contents in olivine are good tracers of melt/fluid metasomatism, whereas Ni/Co, Ni/Mn and Mn/Zn ratios are indicators of chromite mineralization. Therefore, trace elements in olivine can be used as chemical proxies to distinguish the origin of various mafic-ultramafic rocks, as well as the processes by which they evolved.

1. Introduction

The composition of mafic-ultramafic rocks and their crystal cargoes provide windows into the composition of Earth's mantle and the nature of crust-mantle interactions. Such rocks occur in a wide range of tectonic settings and preserve significant records of mantle evolution, magma generation and magma differentiation (e.g., Dawson, 2002; Li et al., 2001). These lithologies can also host significant Ni-PGE-Cr deposits (Kelemen et al., 1998; Pearson et al., 2003; Scoon and Klerk, 1987), and have therefore long been the target of scientific investigations.

Olivine, being the most common and abundant mineral in mafic-ultramafic rocks, is widely used as geophysical and geochemical indicators. For instance, the preferred orientation of olivine crystals can result in seismic anisotropy of the mantle (Jung et al., 2008; Nishimura and Forsyth, 1989), whereas the modal abundance and forsterite (Fo) content of olivine may reflect variable degrees of mantle melting, the nature and evolution of primitive mantle-derived melts (e.g., Bernstein et al., 2007; Herzberg, 2011), as well as the magmatic processes that may influence the composition of basaltic melts during transport to the surface (e.g., Gleeson and Gibson, 2019; Hole, 2018). However, compared to its major elements, studies on the trace element chemistry of olivine are limited.

* Corresponding authors at: Key Laboratory of Mineral Resources, Institute of Geology and Geophysics, Chinese Academy of Sciences, Beijing 100029, China.
E-mail addresses: wangjing@mail.iggcas.ac.cn (J. Wang), subenxun@mail.igcas.ac.cn (B.-X. Su).

https://doi.org/10.1016/j.lithos.2021.106085
0024-4937/

With continued advances in micro-analytical techniques, trace elements in olivine can be precisely measured, thereby attracting increasing attention (Batanova et al., 2015; Brett et al., 2009; De Hoog et al., 2010; Prelević et al., 2013; Sobolev et al., 2008; Su et al., 2019a; Wang et al., 2020). Such data have been used as petrogenetic tracers of mantle source compositions (Gleeson and Gibson, 2019; Herzberg, 2011; Howarth and Harris, 2017; Sobolev et al., 2005), and geothermometry (Bussweiler et al., 2017; Foley et al., 2013; Gavrilenko et al., 2016; Wan et al., 2008), as well as crustal recycling and carbonatitic metasomatism (Foley et al., 2013; Jaques and Foley, 2018; Prelević et al., 2013). However, the study of trace element chemistry of olivine in mafic-ultramafic rocks is still at an early stage. Here we provide in-situ trace element ^{7}Li, ^{27}Al, ^{29}Si, ^{31}P, ^{43}Ca, ^{45}Sc, ^{49}Ti, ^{51}V, ^{53}Cr, ^{55}Mn, ^{59}Co, ^{60}Ni, and ^{66}Zn analyses of olivine crystals from a diverse range of mafic-ultramafic rocks, and use these data to develop geochemical discriminators for their host rocks and to reveal their petrogenesis and related mineralization.

2. Samples

The olivine grains investigated in this study are from a diverse spectrum of mafic-ultramafic samples, including: (i) mantle xenoliths (112 analyses); (ii) ophiolitic peridotites (313 analyses); (iii) layered intrusive rocks (245 analyses); and (iv) Alaskan-type intrusive rocks (136 analyses). The locations of these samples are shown in Fig. 1, and salient features of the sample localities and petrological characteristics are provided below.

2.1. Mantle xenoliths

The mantle xenoliths were collected from Jingyu (North China Craton), Thrace Basin (NW Turkey in the southern margin of the Eurasian continent) and Lashaine (Tanzanian Craton). They all represent fragments of the continental lithospheric mantle. The xenoliths from Jingyu and Thrace Basin are all spinel peridotites, such as lherzolites and harzburgites, with some dunites in the latter; and their petrographic descriptions are available in Tang et al. (2012), and in Aldanmaz et al. (2005) and Jing et al. (2018), respectively.

The Lashaine xenoliths are mainly garnet peridotites, including harzburgites and lherzolites. Harzburgites are mainly composed of light-green olivine, brown orthopyroxene, rosy garnet and brown primary chromian spinel. Apatite and calcite are also observed. Harzburgites usually show protogranular textures with reaction feature especially between garnet and olivine. Olivine grains generally occur as coarse grain, up to 1 cm in diameter, occasionally as inclusions in primary spinel and as moderate and possibly relict grain within garnet aggregate. Some relict orthopyroxenes were found in melt pockets and fine-grained orthopyroxenes occur as the products of reaction in reaction rims. Garnet occurs as aggregate up to 2 cm in diameter and exhibits reaction and/or breakdown texture. Apatite occurs as veins along the olivine boundary and reaching breakdown garnet.

The Lashaine lherzolites are composed predominantly of olivine, orthopyroxene, clinopyroxene, garnet and brown primary chromian spinel. Phlogopite and apatite coexisting with secondary spinel occur in melt pockets together (Dawson, 2002). Calcite is present as vein among silicate minerals and as fine grain in melt pockets. Lherzolite

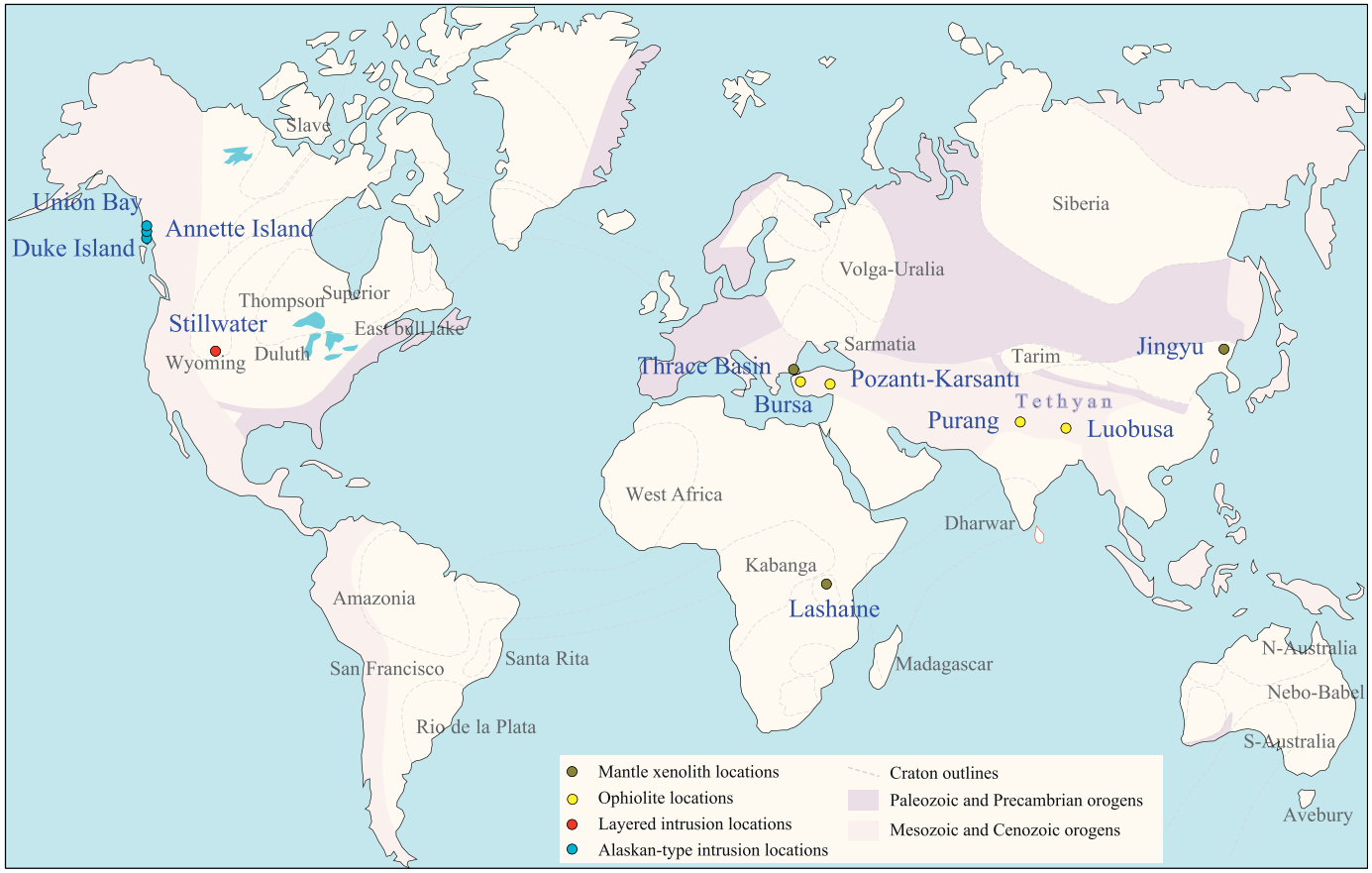

Fig. 1. Locations of the studied mantle xenoliths, ophiolites, layered intrusions and Alaskan-type intrusions. The orogens and fields of cratons are based on Maier and Groves (2011).

displays coarse granular texture and its constituent minerals have slightly curved and straight grain boundaries. Olivine grains vary between 2 and 6 mm in diameter, and occur within garnet and orthopyroxene grains (Rudnick et al., 1994). Fine-grained orthopyroxenes occur as the products in reaction rim where relict olivines are occasionally present. Melting features are also present in sieve-tectured clinopyroxene and primary spinel. Garnets occur as discrete coarse grains and are generally surrounded by reaction rims between garnet and olivine. Most of the secondary spinel grains in melt pockets occur as inclusions in clinopyroxenes.

2.2. Ophiolites

The studied ophiolitic peridotites within the manlte sequences are from the Bursa and Pozantı-Karsantı ophiolites in Turkey (Chen et al., 2020; Liu et al., 2018, 2019; Su et al., 2018), and the Luobusa and Purang ophiolites in China (Su et al., 2015b, 2019b; Xiao et al., 2016). These ophiolites are relics of oceanic lithosphere formed in various spreading centers and stages in the Neo-Tethyan ocean. All the ophiolites but Purang host economic chromite deposits. The studied ophiolitic olivine grains were mainly selected from the least-altered harzburgites, dunites, and chromitites, with additional lherzolites of the Purang ophiolite.

2.3. Layered intrusions

The layered intrusive rocks were collected from the Peridotite Series of the Stillwater Complex in the Wyoming Craton, which hosts world-class stratiform chromite and PGE deposits (Jackson, 1961). The studied samples are composed of olivine, olivine + orthopyroxene, and olivine + chromite, termed dunite, harzburgite and chromitite, respectively (Bai et al., 2019, 2021). They are representative of the entire vertical stratigraphic section of the Peridotite Series and, thus, represent the early formation stage of a large layered intrusion.

2.4. Alaskan-type intrusions

Alaskan-type intrusive rocks were collected from three localities, namely Duke Island, Annette Island, and Union Bay in southeastern Alaska. The samples from Duke Island are composed chiefly of dunite and olivine clinopyroxenite, and their petrological and geochemical features have been described by Liang (2018) and Thakurta et al. (2008). The other two intrusions consist mainly of dunite and wehrlite, with additional olivine clinopyroxenite and gabbro in Union Bay (Liang, 2018; Ruckmick and Noble, 1959).

As the mantle xenoliths are mantle residues after partial melting, and ophiolitic peridotites formed by partial melting and later melt-peridotite interaction, we define the olivine from these bodies as residual olivine, whereas the layered and Alaskan-type intrusions are fractional crystallization products within crustal depth, their olivine is referred to magmatic olivine.

3. Analytical techniques

3.1. Major element analyses

Major and minor elements of olivine were determined by wavelength dispersive spectrometry using a JEOL JXA8100 electron probe microanalyzer (EPMA) at the Institute of Geology and Geophysics, Chinese Academy of Sciences, Beijing. Each olivine grain was analyzed at 15 kV accelerating voltage, 10 nA beam current and 5 μm beam spot. Peak and background counting times for major elements Mg, Si and Fe were 20 s and 10 s, respectively, whereas 60 s and 30 s were used for minor elements, such as Mn and Ni. Natural and synthetic minerals were used for standard calibration. A program based on the ZAF procedure was used for matrix corrections. Typical analytical uncertainties for all the elements analyzed were better than 1–2%.

3.2. Trace element analyses

Trace elements were measured by a 193 nm excimer laser (RESOlution M-50, ASI) coupled to an inductively coupled plasma mass spectrometer (Agilent 7900) at the State Key Laboratory of Continental Dynamics in Northwest University. The operating conditions and procedures are described in detail by Bao et al. (2016). Each analysis was performed using 60-μm-diameter ablating spots at 6 Hz with energy of ~100 mJ per pulse for 45 s after measuring the gas blank for 20 s. The following isotopes were measured: ^{7}Li, ^{27}Al, ^{29}Si, ^{31}P, ^{43}Ca, ^{45}Sc, ^{49}Ti, ^{51}V, ^{53}Cr, ^{55}Mn, ^{59}Co, ^{60}Ni, and ^{66}Zn.

A glass standard, NISTSRM 610, was used for external calibration, and BCR-2G and BHVO-2G standards were used to monitor instrument drift. Off-line data processing was performed with the ICPMSDataCal10.9 program using ^{29}Si as an internal standard. The accuracy was in a discrepancy of ±10%, with the analytical precision less than 10% for ^{7}Li, ^{27}Al, ^{29}Si, ^{31}P, ^{45}Sc, ^{49}Ti, ^{51}V, ^{53}Cr, ^{55}Mn, ^{59}Co, ^{60}Ni and ^{66}Zn, and between 10 and 15% for ^{43}Ca. Analytical results of NISTSRM 610, BCR-2G and BHVO-2G are consistent with their recommended values, and olivine trace element data of samples numbered '06JY' obtained by ICP-MS and LA-ICP-MS are in good agreement (Supplementary Table 1; Wang et al., 2020). Major and trace element data of the individual olivine grains are all presented in Supplementary Table 2.

4. Results

The olivine grains from mantle xenoliths have Fo contents ranging from 87 to 96 (Supplementary Table 2), consistent with those in continental lithospheric mantle (Bernstein et al., 2007; Boyd, 1989). Their Ni (2610–3336 ppm), Ca (<732 ppm), Cr and Al (<300 ppm), Li, V and Sc contents (<10 ppm) are within ranges previously determined for mantle xenolithic olivine, whereas Mn contents (554–1483 ppm) are slightly higher (De Hoog et al., 2010; Simkin and Smith, 1970; Sobolev et al., 2009). Titanium and P contents of the mantle xenolithic olivine both vary from 1 to 216 ppm. Their Co and Zn contents range from 115 to 160 ppm and 40 to 113 ppm, respectively, higher than estimated primary mantle (PM) values (McDonough and Sun, 1995).

Olivine grains from ophiolitic peridotites have Fo values from 89 to 96, with Ni (1280–4365 ppm) and Mn (512–1786 ppm) contents (Fig. 2a, b) in the same ranges of ophiolites reported by Chen et al. (2019). Their Co (61–186 ppm), Zn (6–72 ppm), Ti (<22 ppm), P (4–30 ppm), and V and Sc (<10 ppm) contents (Fig. 2c, d, f, i, k, l) are within the range of olivine from Alpine Jurassic ophiolites (Sanfilippo et al., 2014), whereas Ca contents are highly variable, ranging from 30 to 1694 ppm (Fig. 2e). Chromium and Al range from 5 to 292 ppm and 2 to 134 ppm, respectively (Fig. 2g, h), and Li contents are <4 ppm (Fig. 2j).

Olivine grains from the layered intrusive rocks have lower Fo values ranging from 83 to 90, within the range of olivine from the Stillwater layered intrusion (Bai et al., 2019, 2021). Their Ni, Mn, Co and Zn contents are 1999–3345 ppm, 1187–2174 ppm, 102–209 ppm and 16–86 ppm (Fig. 2a–d), respectively. The olivine grains have Ca contents of 71–631 ppm, and Ti (5–62 ppm) and P (9–201 ppm) contents are slightly low (Fig. 2e, f, i). Their Cr and Al contents are <100 ppm, whereas the Li, V and Sc contents are <7 ppm, < 4 ppm and 2–6 ppm, respectively (Fig. 2g, h, j–l).

The Alaskan-type intrusive rocks have olivine with Fo values in the range of 78–90, and their Ni (332–2024 ppm), Mn (1212 to 3971 ppm) and Ca contents (30 to 2044 ppm) are consistent with olivine values reported for the Duke island and Xiadong Alaskan-type intrusions (Bai et al., 2017; Himmelberg and Loney, 1995; Li et al., 2012, 2013). The olivine Co (125 to 289 ppm), Zn (32 to 177 ppm), Al (2 to 338 ppm) and Cr contents (2–230 ppm) in these rocks are highly

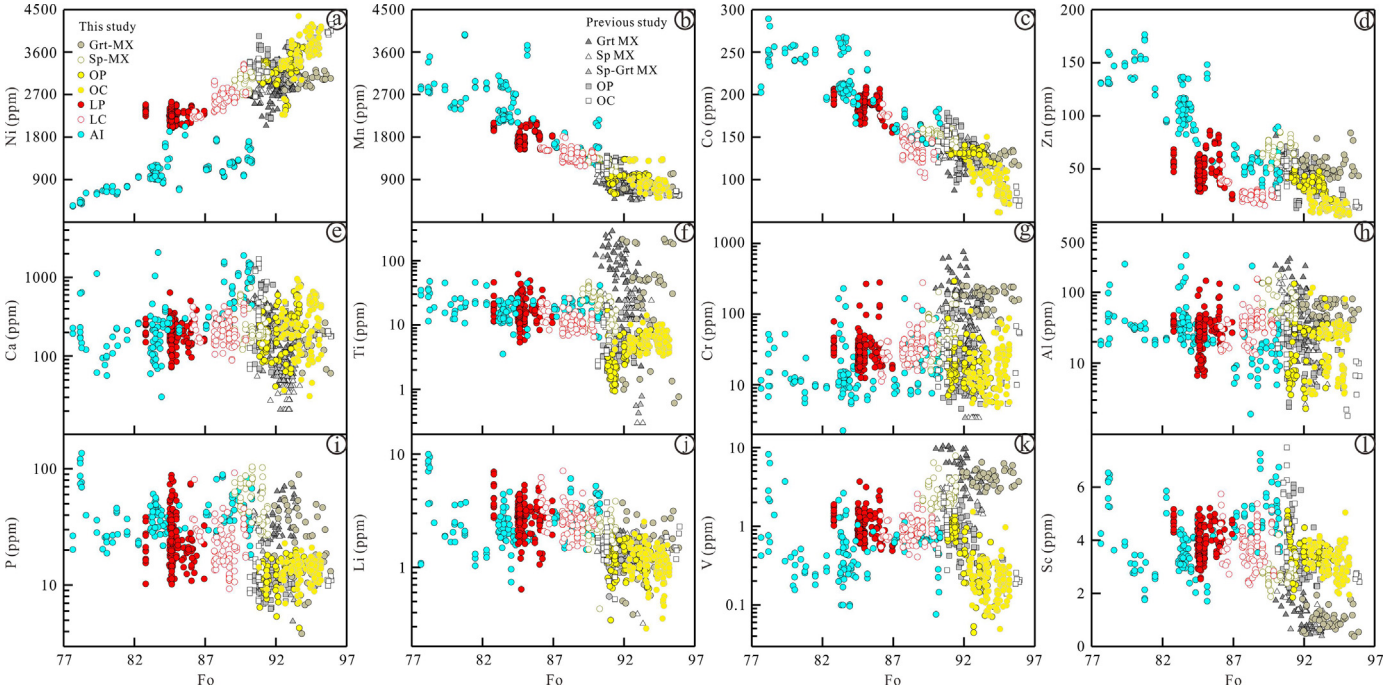

Fig. 2. Element contents (ppm) versus forsterite (Fo) value of olivine (a-l). Samples are from mantle xenoliths (garnet peridotites, Sp-Grt peridotites and spinel peridotites), ophiolites (peridotites and chromitites), layered intrusive rocks (peridotites and chromitites) and Alaskan-type intrusive rocks. Grt-MX: garnet peridotites; Sp-MX: spinel peridotites; OP: ophiolitic peridotites; OC: ophiolitic chromitites; LP: layered intrusive peridotites; LC: layered intrusive chromitites; AI: Alaskan-type intrusive rocks. Fo values of olivine in mantle xenoliths are from Jing et al. (2018), Su et al. (2015a), and this study; values for ophiolites are from Chen et al. (2020) and Su et al. (2018, 2019b); values for layered intrusions are from Bai et al. (2019, 2021), and for Alaskan-type intrusions are from Liang (2018) and this study. Trace elements compositions of olivine in ophiolites are from Su et al. (2019b) and Chen et al. (2020), mantle xenoliths are from Sobolev et al. (2009) and De Hoog et al. (2010).

variable (Fig. 2c, d, g, h). Their Ti and P contents are within the ranges of 4–48 ppm and 19–138 ppm, respectively, whereas the Li, V and Sc contents are all <10 ppm (Fig. 2f, i–l).

5. Discussion

Olivine is one of the most refractory minerals present during partial melting of mantle peridotites, and it is also the first silicate mineral to crystallize from most mantle-derived melts (Bowen, 1928; Kushiro, 1975). Olivine crystals from mantle residues preserve the chemical signatures of melt loss in peridotites (Bernstein et al., 2007; De Hoog et al., 2010), whereas the olivine grains crystallized from the mantle-derived melts record the earliest stage of evolving mantle-derived magmas and processes occurring in crustal magma storage chambers (Gleeson and Gibson, 2019; Hole, 2018; Jaques and Foley, 2018; Lynn et al., 2018). Therefore, olivine is an excellent monitor of the chemistry of mantle residues and magma differentiation.

5.1. Trace element variations in mantle residual olivine: Differences of mantle melting and metasomatism between continental and oceanic lithospheric mantle

A variety of petrological and geophysical studies have revealed that the mantle xenoliths are residues of continental lithospheric mantle, which is likely to have a maximum thickness of 250 km (Anderson, 1994; Forte and Perry, 2000) and melts under high temperatures (Foley et al., 2013). On the other hand, ophiolites form in a variety of tectonic environments and are considered to be residues of the oceanic lithospheric mantle (Su et al., 2018; Winter, 2013).

Olivine grains from spinel peridotites have similar Ni and higher Mn, Co and Zn than those from garnet peridotites; however, they have similar Ni, Mn and Co contents but higher Zn compared to the ophiolitic olivine at a given Fo and overlap with each other (Figs. 2a–c, 4a, b). The higher Mn and Co contents in olivine from spinel peridotites compared to those from garnet peridotites show that the partition coefficient of these elements decreases at elevated temperatures, which is consistent with the partitioning between olivine and melt during partial melting (Davis et al., 2013; Le Roux et al., 2011). The similar Ni contents show that its partitioning is controlled not only by temperature, but also by the modal abundance of olivine in the residual mantle (Matzen et al., 2013, 2017). Therefore, the Ni/Co and Ni/Mn ratios are slightly fractionated between the spinel peridotites, garnet peridotites and ophiolitic peridotites (Fig. 4e, f).

Olivine grains in mantle xenoliths have similar Ca, but higher Ti, Cr, Al, P and Li contents at a given Fo value compared to ophiolitic olivine (Fig. 2f–j), indicating relatively low degrees of partial melting of the mantle xenoliths compared to ophiolitic peridotites; an observation consistent with their mineral assemblages. The distribution of Ca in the residual olivine is related to its partition coefficient between olivine and melt, which is similar in garnet and spinel peridotites but decreases with increasing H_2O (Gavrilenko et al., 2016). The distribution of Li appears to be virtually independent of temperature, pressure and mineral composition (Mallmann et al., 2009) but it has high fluid activities, and thus the large range of Li contents in olivine from mantle xenoliths may be related to metasomatic processes, as suggested by earlier workers (Dawson, 2002; Gibson et al., 2013; Jing et al., 2018). Similar changes in Ti and P with Fo may also reflect the metasomatism.

Olivine grains from spinel peridotites have lower V and higher Sc compared to those from garnet peridotites but higher V and similar Sc contents compared to ophiolitic olivine (Figs. 2g, k, l, 4c, d). In addition, the two lithologies can be easily distinguished by their olivine V/Sc ratios (Fig. 4f). Vanadium is a polyvalent cation that occurs as V^{3+} or V^{4+} at terrestrial values of oxygen fugacity (fO_2) (Borisov et al., 1987). As the crystal structures of most phases on the liquidus of mafic and ultramafic magmas preferentially incorporate V^{3+} over V^{4+}, the $D_V^{olivine/liq}$ typically decreases with increasing fO_2 (Canil,

1997; Canil and Fedortchouk, 2001). The higher V content of olivine grains from the mantle xenoliths may be attributed to a relatively low fO_2 of the continental lithospheric mantle relative to the oceanic lithospheric mantle (Canil, 2002; Canil and Fedortchouk, 2000), which most likely experienced metasomatism from subduction-related fluids/melts prior to emplacement.

The behavior of Sc is typically considered to be similar to V during mantle melting, but it is not redox-sensitive (Laubier et al., 2014; Lee et al., 2005; Mallmann and O'Neill, 2009). Sc in olivine is less compatible than in garnet (Davis et al., 2013; De Hoog et al., 2010). As a result, Sc contents are lower in olivine from garnet peridotites than olivine from spinel peridotites. V/Sc ratio can serve as a proxy for the oxidation state during partial melting based on the principle that the major difference in V/Sc ratio of the resulting melt/residue is driven by changes in oxidation state rather than melt-fraction or other melting processes (Canil and Fedortchouk, 2001; Zanetti et al., 2004).

5.2. Trace element fractionation during magma differentiation and mineralization

Layered intrusions are typically found in ancient cratons and exhibit evidence of extensive fractional crystallization and crystal segregation by settling or floating of minerals in a melt, which are ascribed to plume magmatism or rift upwelling (Wager and Brown, 1968), whereas Alaskan-type intrusions, which typically occur in orogenic belts, consist of a dunite core, surrounded by wehrlite, clinopyroxenite, hornblendite, and gabbro zones concentrically arranged outward, which are products of post-accretion, island arc or active continental margin magmatism (Noble, 1960; Taylor, 1967; Cui et al., 2020). Therefore, the trace element contents in olivine are principally controlled by the tectonic setting and co-crystallizing minerals, such as orthopyroxene, clinopyroxene and chromite.

Nickel, Mn, Co and Zn concentrations in magmatic olivine generally correlate with Fo values, which is consistent with fractional crystallization (Fig. 2a-d). In olivine, Ni ($D_{Ni}^{Ol/melt} = 5.65–10.28$) is a highly compatible element, whereas Co, Zn and Mn ($D_{Co}^{Ol/melt} = 1.96–3.08$, $D_{Zn}^{Ol/melt} = 0.89–1.16$ and $D_{Mn}^{Ol/melt} = 0.75–1.15$, respectively) show less compatible behavior, and they are more compatible than other rock-forming minerals, such as orthopyroxene ($D_{Ni}^{Opx/melt} = 2.77–4.49$, $D_{Co}^{Opx/melt} = 0.89–1.46$, $D_{Zn}^{Opx/melt} = 0.6–0.77$ and $D_{Mn}^{Opx/melt} = 0.66–1.05$) and clinopyroxene ($D_{Ni}^{Cpx/melt} = 2.44–3.78$, $D_{Co}^{Cpx/melt} = 0.96–1.18$ and $D_{Zn}^{Cpx/melt} = 0.44–0.5$), except Mn ($D_{Mn}^{Cpx/melt} = 1.06–1.16$) (Davis et al., 2013; De Hoog et al., 2010; Le Roux et al., 2011). Olivine grains in the layered intrusive rocks show narrower variations in Fo, Mn, Co and Zn than those in the Alaskan-type intrusive rocks, due to the lower evolvement.

The Ni/Co and Ni/Mn ratios in olivine from the layered intrusive rocks rarely fractionate, whereas the Ni/Co, Ni/Mn and Mn/Zn ratios in olivine from the Alaskan-type intrusive rocks decrease with Fo (Fig. 3), which may be related to the coexisting mineral, orthopyroxene and clinopyroxene, respectively, and consistent with previous study that the crystallization of olivine and orthopyroxene do not significantly fractionate Ni/Co but clinopyroxene can fractionate Ni/Co and Mn/Zn (Le Roux et al., 2011). However, olivine grains in the layered intrusive rocks show higher Ni at a given Fo than olivine in the Alaskan-type intrusive rocks (Figs. 2a, d, 3a, b), indicating that the primary differences between the layered intrusions and Alaskan-type intrusions are not only related to the degree of fractional crystallization but also to the tectonic setting. The Alaskan-type intrusions are products of arc magma, which referred to a low temperature; however, layered intrusions are related to mantle plume which has higher temperature, and thus the contents of partial melts have high concentration of Ni because of the negative effect of temperature on the D^{Ol-liq} of Ni (Li and Ripley, 2010).

Incompatible elements in magmatic olivine show relatively little variations with Fo (Fig. 2e–l). Olivine grains in the layered intrusive rocks have lower Zn and P, but higher Cr and V contents at a given Fo

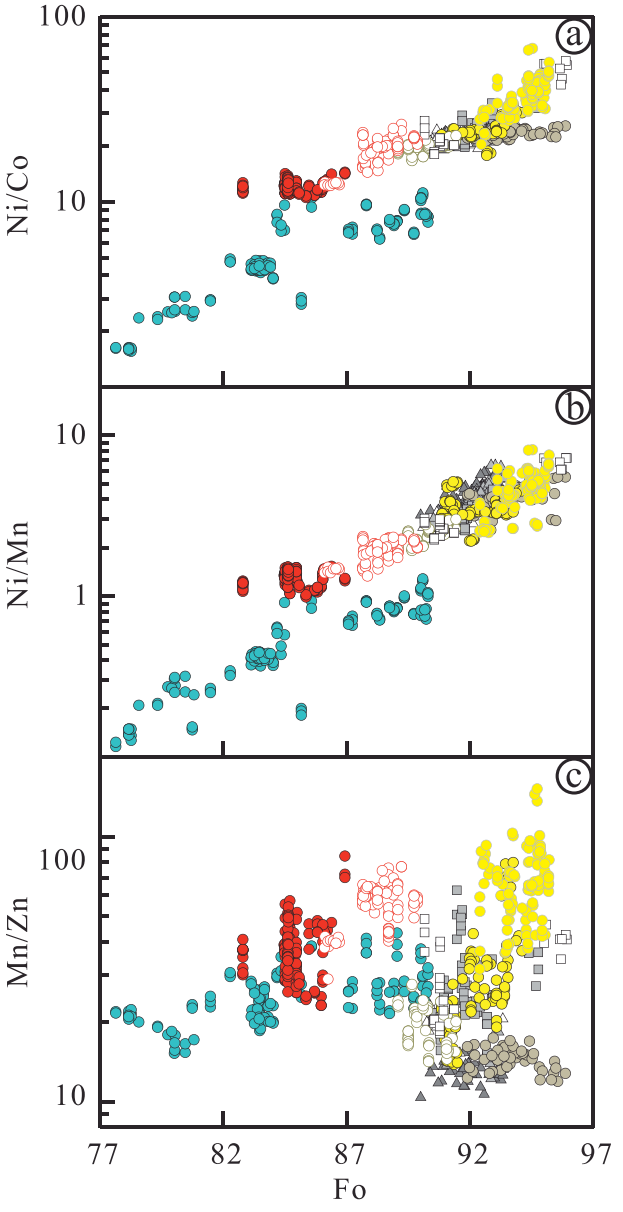

Fig. 3. Trace element ratios versus Fo of olivine. (a) Ni/Co vs. Fo, (b) Ni/Mn vs. Fo and (c) Mn/Zn vs. Fo. Samples are from mantle xenoliths (garnet peridotites, Sp-Grt peridotites and spinel peridotites), ophiolites (peridotites and chromitites), layered intrusive rocks (peridotites and chromitites) and Alaskan-type intrusive rocks. Data sources and symbols are same as in Fig. 2.

than those in the Alaskan-type intrusive rocks (Fig. 2d, g, i, k), which may be related to the mantle sources. The layered intrusions are products of partial melting of peridotites in the continental lithospheric mantle, which have a relatively low fO_2 than the oceanic lithospheric mantle as aforementioned (Canil, 2002; Canil and Fedortchouk, 2000), and thus olivine grains in the layered intrusions have higher Cr and V contents. The primary magma of the Alaskan-type intrusions was derived from fluids/melts metasomatized mantle wedge in a subduction zone setting (e.g., Himmelberg and Loney, 1995; Murray 1972; Cui et al., 2020), which resulted in the enrichment of elements, such as Zn and P.

Olivine grains in chromitites from the ophiolites and layered intrusions both have higher Fo and Ni, but lower Mn, Co, Zn contents than olivine from the peridotites (Fig. 2a–d). Thus, the Ni/Co, Ni/Mn and Mn/Zn ratios can be used to trace the mineralization of chromite (Figs. 3a–c, 4e,

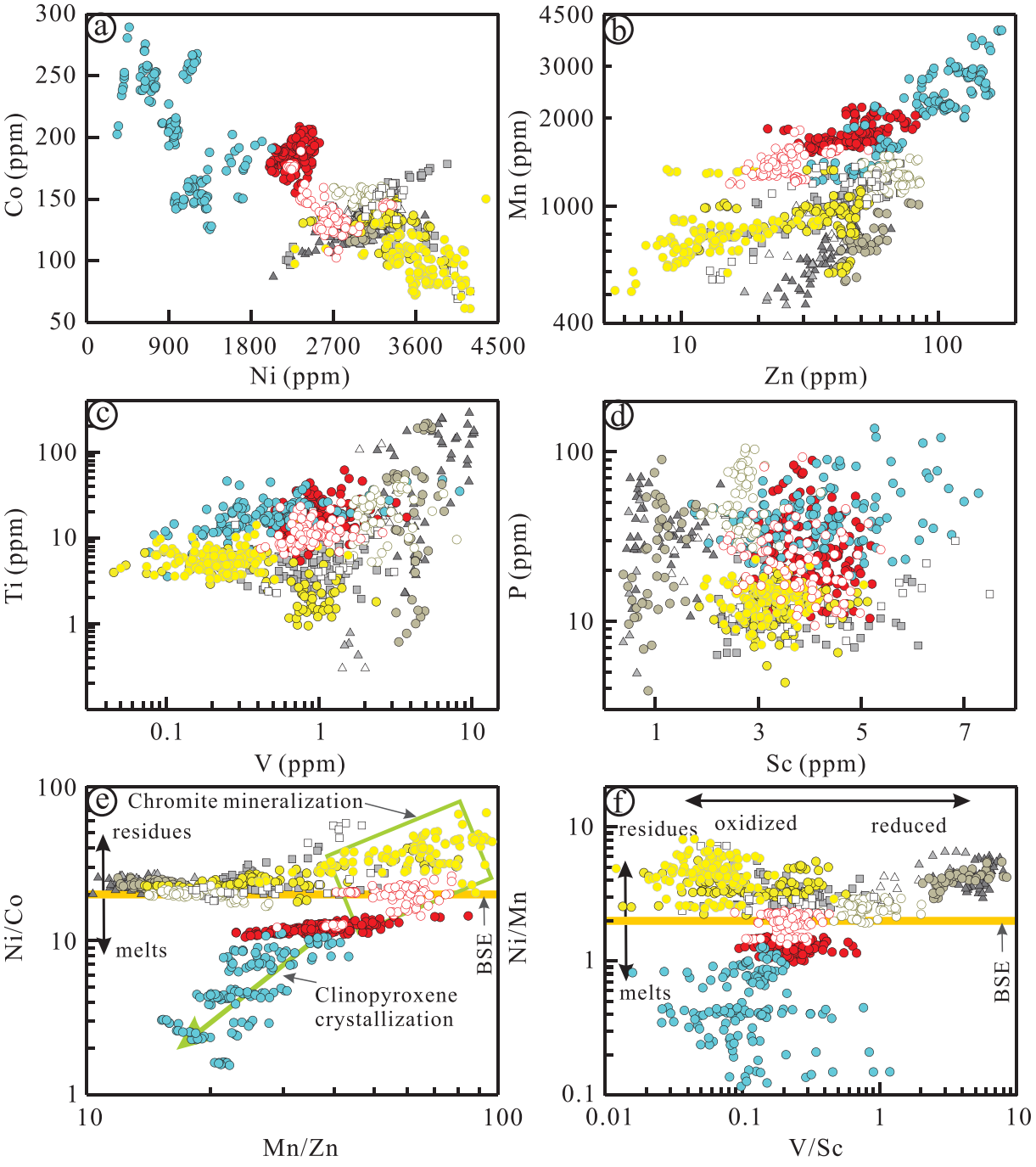

Fig. 4. Trace element chemistry of the olivine analyzed in the mantle xenoliths, ophiolites, layered intrusions and Alaskan-type intrusions. (a) Ni vs. Co and (b) Zn vs. Mn can be used to discriminate the mantle residues from melts. (c) V vs. Ti and (d) Sc vs. P diagrams are suitable to discriminate between continental lithospheric mantle and oceanic lithospheric mantle. (e) Mn/Zn vs. Ni/Co, and Ni/Co = 20 ± 1 represents bulk silicate Earth (BSE) (McDonough and Sun, 1995), whereas olivine crystals from mantle residues are >20 but <20 for magmatic olivine. (f) V/Sc vs. Ni/Mn, V/Sc ratios can be used to characterize the oxidation state, which decrease with increasing oxidation, but increase with increasing reduction. Ni/Mn = 2 represents bulk silicate Earth (BSE) (McDonough and Sun, 1995). Data sources and symbols are same as in Fig. 2.

f). As previous studied, Ni ($D_{Ni}^{Sp/melt}$ = 1.3–3.2) is less compatible in chromite compared to olvine, whereas Mn ($D_{Mn}^{Sp/melt}$ = 2.1), Co (3.83–4.49) and Zn (6.9–7.92) are more compatible (Foley et al., 2013; Pagé and Barnes, 2009). Therefore, the crystallization of chromite consumes Mn, Co and Zn, and increase the Ni/Co, Ni/Mn and Mn/Zn ratios in olivine (Figs. 3a–c, 4e, f), supported by the covariations of trace elements between olivine and chromite in previous studies (Su et al., 2019b). The higher Fo could be attributed to Fe—Mg exchange between olivine and chromite (Bai et al., 2017, 2021; Xiao et al., 2016).

5.3. Trace element discrimination for mafic-ultramafic rocks

Distinct Ni, Co and Mn contents in olivine can be employed to classify the host mafic-ultramafic rocks into two groups, made up of: (i) mantle xenoliths and ophiolites and (ii) layered and Alaskan-type intrusive rocks, which, respectively, represent mantle residues and mantle-derived melts (Figs. 2a–c, 4a, b). Nickel is a highly compatible element in olivine compared to other mantle minerals and tends to be retained in residues during partial melting,

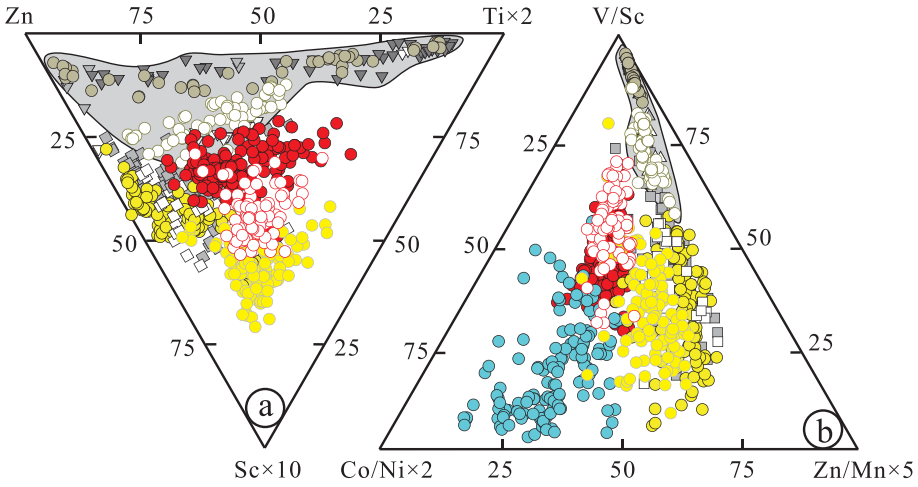

Fig. 5. Ternary diagram of (a) (Sc × 10)-(Ti × 2)-Zn, olivine grains in the mantle xenoliths are characterized by the lowest percentage of Sc × 10, whereas olivine grains in the ophiolites show a higher percentage of Sc × 10 but lower Ti × 2 compared to olivine in the layered intrusions. (b) V/Sc-(Co/Ni × 2)-(Zn/Mn × 5), olivine grains in the mantle xenoliths show the lowest Co/Ni × 2 and Zn/Mn × 5 but the highest V/Sc, whereas olivine in the ophiolites and layered intrusions are characterized by a middle percentage of V/Sc and Co/Zn × 2. Olivine in Alaskan-type intrusions shows the highest Co/Ni × 2. Data sources and symbols are same as in Fig. 2

whereas Co and Mn show compatible to slightly incompatible behavior during mantle melting (Davis et al., 2013; Le Roux et al., 2011), leading to lower concentrations in residual olivine compared to those in magmatic olivine.

Nickel, Co and Mn are not influenced by metasomatism, and thus, Ni/Co and Ni/Mn ratios can be used to distinguish between mantle melting and magma fractionation. The Ni/Co and Ni/Mn ratios in residual olivine (> 20 and > 2, respectively) are higher than the bulk silicate earth (BSE) values (McDonough and Sun, 1995), and consistent with values reported in earlier studies (Sobolev et al., 2007), whereas magmatic olivine shows lower Ni/Co and Ni/Mn ratios (<20 and <2, respectively) (Figs. 3a, b, 4e, f). Elements such as Zn, Ti, V and Sc, and V/Sc ratio in residual olivine show different ranges, making them distinct discriminators between mantle xenolithic olivine, ophiolitic olivine or both (Figs. 2d, f, k, l, 4f).

We combine these values and ratios, and propose discriminations empirically rather than statistically, in order to produce diagrams that can be understood in petrogenetic terms. The contents of Sc and Ti were magnified to the same order of magnitude as Zn, whereas the ratios of Co/Ni and Zn/Mn were magnified to the same order of magnitude as V/Sc before they were converted to percentages so that they could be separated significantly (Fig. 5).

The Sc × 10 of olivine grains from the mantle xenoliths are below 30%, whilst Ti × 2 and Zn both show a wide range from 0 to 90% in the ternary diagram (Fig. 5a). The ophiolitic olivine grains are characterized by higher percentages of Sc × 10 (30–70%) compared to olivine grains from the mantle xenoliths and show the lowest Ti × 2 (below 35%) values. The olivine grains from layered intrusions are scattered in the middle part of the ternary diagram and form a separated field distinct from olivine in mantle xenoliths, with the narrow range of Sc × 10 (23–53%) and Ti × 2 (below 20–37%), respectively.

Olivine grains from the mantle xenoliths are characterized by the lowest ratios of Co/Ni × 2 (< 14%) and Zn/Mn × 5 (< 30%) and the highest V/Sc (60–95%) (Fig. 5b), whereas olivine grains from the ophiolitic peridotites show a higher Co/Ni × 2 (10–40%) and Zn/Mn × 5 (28–60%) and lower V/Sc percentage (10–62%). The olivine grains from the layered intrusions still plot in the middle part of the ternary diagram with percentages of 20–37% Co/Ni × 2, 16–32% Zn/Mn × 5 and 37–63% V/Sc. Olivine grains from the Alaskan-type intrusions have the lowest percentage of V/Sc (5–42%) and the highest Co/Ni × 2 (43–78%). All the mafic-ultramafic rocks can be discriminated by the ternary diagram of V/Sc-(Co/Ni × 2)-(Zn/Mn × 5) (Fig. 5b).

6. Conclusions

This study presents new analyses of trace elements in olivine from mantle xenoliths, ophiolites, layered intrusions and Alaskan-type intrusions. The following conclusions could be drawn:

(1) Olivine grains from mantle xenoliths and ophiolitic peridotites have higher Ni/Co (>20) and Ni/Mn (>2) ratios compared to magmatic olivine from layered and Alaskan-type intrusions, whereas olivine grains from the Alaskan-type intrusions have lower Ni/Mn and Ni/Co ratios than those from the layered intrusions.
(2) Olivine grains from the mantle xenoliths have higher V contents (>2 ppm) and V/Sc ratios (>0.5) compared to those in the ophiolitic peridotites, indicating that the oxygen fugacity of the continental lithospheric mantle is lower than that of the oceanic lithospheric mantle.
(3) Olivine grains from mantle xenoliths, ophiolites, the layered intrusions and Alaskan-type intrusions can be distinguished by (Sc × 10)-(Ti × 2)-Zn and V/Sc-(Co/Ni × 2)-(Zn/Mn × 5) discriminant diagrams. In addition, the elevated Ni/Co, Ni/Mn and Mn/Zn ratios represent indicators of chromite mineralization.

Supplementary data to this article can be found online at https://doi.org/10.1016/j.lithos.2021.106085.

Declaration of Competing Interest

The authors declare that they have no known competing financial interests or personal relationships that could have appeared to influence the work reported in this paper.

Acknowledgements

This study was financially supported by the National Natural Science Foundation of China (Grants 41973012, 91755205 and 41772055), and Youth Innovation Promotion Association, Chinese Academy of Sciences.

References

Aldanmaz, E., Gourgaud, A., Kaymakcı, N., 2005. Constraints on the composition and thermal structure of the upper mantle beneath NW Turkey: evidence from mantle xenoliths and alkali primary melts. J. Geodyn. 39, 277–316.

Anderson, D.L., 1994. The sublithospheric mantle as the source of continental flood basalts; the case against the continental lithosphere and plume head reservoirs. Earth Planet. Sci. Lett. 123, 269–280.
Bai, Y., Su, B.X., Chen, C., Yang, S.H., Liang, Z., Xiao, Y., Qin, K.Z., Malaviarachchi, S.P.K., 2017. Base metal mineral segregation and Fe-Mg exchange inducing extreme compositions of olivine and chromite from the Xiadong Alaskan-type complex in the southern part of the Central Asian Orogenic Belt. Ore Geol. Rev. 90, 184–192.
Bai, Y., Su, B.X., Xiao, Y., Chen, C., Cui, M.M., He, X.Q., Qin, L.P., Charlier, B., 2019. Diffusion-driven chromium isotope fractionation in ultramafic cumulate minerals: elemental and isotopic evidence from the Stillwater complex. Geochim. Cosmochim. Acta 263, 167–181.
Bai, Y., Su, B.X., Xiao, Y., Cui, M.M., Charlier, Bernard, 2021. Magnesium and iron isotopic evidence of inter-mineral diffusion in ultramafic cumulates of the Peridotite Zone, Stillwater Complex. Geochim. Cosmochim. Acta 292, 152–169.
Bao, Z.A., Yuan, H.L., Zong, C.L., Liu, Y., Chen, K.Y., Zhang, Y.L., 2016. Simultaneous determination of trace elements and lead isotopes in fused silicate rock powders using a boron nitride vessel and fsLA-(MC)-ICP-MS. J. Anal. At. Spectrom. 31, 1012–1022.
Batanova, V.G., Sobolev, A.V., Kuzmin, D.V., 2015. Trace element analysis of olivine: High precision analytical method for JEOL JXA-8230 electron probe microanalyser. Chem. Geol. 419, 149–157.
Bernstein, S., Hanghøj, K., Kelemen, P.B., 2007. Consistent olivine Mg# in cratonic mantle reflects Archean mantle melting to the exhaustion of orthopyroxene. Geology 35, 459–462.
Borisov, A.A., Kadik, A.A., Zharkova, Y.V., Kalinichenko, N.V., 1987. Effects of oxygen fugacity on the ratio between valency forms of vanadium in magmas. Geochem. Int. 24, 15–20.
Bowen, N.L., 1928. The evolution of igneous rocks. Sci. Prog. 1, 152–165.
Boyd, F.R., 1989. Compositional distinction between oceanic and cratonic lithosphere. Earth Planet. Sci. Lett. 96, 15–26.
Brett, R.C., Russell, J.K., Moss, S., 2009. Origin of olivine in kimberlite: Phenocryst or impostor? Lithos 112, 201–212.
Bussweiler, Y., Brey, G.P., Pearson, D.G., Stachel, T., Stern, R.A., Hardman, M.F., Kjarsgaard, B.A., Jackson, S.E., 2017. The Aluminum-in-olivine thermometer for mantle peridotites-Experimental versus empirical calibration and potential applications. Lithos 272-273, 301–314.
Canil, D., 1997. Vanadium partitioning and the oxidation state of Archaean komatiite magmas. Nature 389, 842.
Canil, D., 2002. Vanadium in peridotites, mantle redox and tectonic environments: Archean to present. Earth Planet. Sci. Lett. 195, 75–90.
Canil, D., Fedortchouk, Y., 2000. Clinopyroxene-liquid partitioning for vanadium and the oxygen fugacity during formation of cratonic and oceanic mantle lithosphere. J. Geophys. Res. Solid Earth 105, 26003–26016.
Canil, D., Fedortchouk, Y., 2001. Olivine-liquid partitioning of vanadium and other trace elements, with applications to modern and ancient picrites. Can. Mineral. 39, 319–330.
Chen, C., Su, B.X., Xiao, Y., Pang, K.N., Robinson, P.T., Uysal, I., Lin, W., Qin, K.Z., Avcı, E., Kapsiotis, A., 2019. Intermediate chromitite in Kızıldağ ophiolite (SE Turkey) formed during subduction initiation in Neo-Tethys. Ore Geol. Rev. 104, 88–100.
Chen, C., De Hoog, J.C.M., Su, B.X., Wang, J., Uysal, İ., Xiao, Y., 2020. Formation processes of dunites and chromitites in Orhaneli and Harmancık ophiolites (NW Turkey): evidence from in-situ Li isotopes and trace elements in olivine. Lithos 376-377, 105773.
Cui, M.M., Bai, Y, Luo, Y, Su, B.X., Xiao, Y., Wang, J., Pan, Q.Q., Guo, D.L., 2020. Characteristics, petrogenesis and metallogenesis of Alaskan-type complexes. Miner. Depos. 39, 397–418 (in Chinese with English abstract).
Davis, F.A., Humayun, M., Hirschmann, M.M., Cooper, R.S., 2013. Experimentally determined mineral/melt partitioning of first-row transition elements (FRTE) during partial melting of peridotite at 3GPa. Geochim. Cosmochim. Acta 104, 232–260.
Dawson, J.B., 2002. Metasomatism and partial melting in upper-mantle peridotite xenoliths from the Lashaine volcano, northern Tanzania. J. Petrol. 43, 1749–1777.
De Hoog, J.C.M., Louise, G., Cornell, D.H., 2010. Trace-element geochemistry of mantle olivine and application to mantle petrogenesis and geothermobarometry. Chem. Geol. 270, 196–215.
Foley, S.F., Prelevic, D., Rehfeldt, T., Jacob, D.E., 2013. Minor and trace elements in olivines as probes into early igneous and mantle melting processes. Earth Planet. Sci. Lett. 363, 181–191.
Forte, A.M., Perry, H.K., 2000. Geodynamic evidence for a chemically depleted continental tectosphere. Science 290, 1940–1944.
Gavrilenko, M., Herzberg, C., Vidito, C., Carr, M.J., Tenner, T., Ozerov, A., 2016. A calcium-in-olivine geohygrometer and its application to subduction zone magmatism. J. Petrol. 57, 1811–1832.
Gibson, S.A., McMahon, S.C., Day, J.A., Dawson, J.B., 2013. Highly refractory lithospheric mantle beneath the Tanzanian Craton: evidence from lashaine pre-metasomatic garnet-bearing peridotites. J. Petrol. 54, 1503–1546.
Gleeson, M.L.M., Gibson, S.A., 2019. Crustal controls on apparent mantle pyroxenite signals in ocean-island basalts. Geology 47, 321–324.
Herzberg, C., 2011. Identification of source lithology in the Hawaiian and Canary islands: Implications for origins. J. Petrol. 52, 113–146.
Himmelberg, G.R., Loney, R.A., 1995. Characteristics and Petrogenesis of Alaskan-Type Ultramafic-Mafic Intrusions, Southeastern Alaska. US Government Printing Office.
Hole, M.J., 2018. Mineralogical and geochemical evidence for polybaric fractional crystallization of continental flood basalts and implications for identification of peridotite and pyroxenite source lithologies. Earth-Sci. Rev. 176, 51–67.
Howarth, G.H., Harris, C., 2017. Discriminating between pyroxenite and peridotite sources for continental flood basalts (CFB) in southern Africa using olivine chemistry. Earth Planet. Sci. Lett. 475, 143–151.
Jackson, E.D., 1961. Primary Textures and Mineral Associations in the Ultramafic Zone of the Stillwater Complex. US Geological Survey, Montana.
Jaques, A.L., Foley, S.F., 2018. Insights into the petrogenesis of the West Kimberley lamproites from trace elements in olivine. Mineral. Petrol. 112, 519–537.
Jing, J.J., Su, B.X., Xiao, Y., Martin, L., Zhang, H.F., Uysal, İ., Chen, C., Lin, W., Chu, Y., Seitz, H.M., Zhang, P.F., 2018. Cryptic metasomatism revealed by Li isotopes of mantle xenoliths beneath the Thrace Basin, NW Turkey. J. Asian Earth Sci. 166, 270–278.
Jung, H., Mo, W., Green, H.W., 2008. Upper mantle seismic anisotropy resulting from pressure-induced slip transition in olivine. Nat. Geosci. 2, 73–77.
Kelemen, P.B., Hart, S.R., Bernstein, S., 1998. Silica enrichment in the continental upper mantle via melt/rock reaction. Earth Planet. Sci. Lett. 164, 387–406.
Kushiro, I., 1975. On the nature of silicate melt and its significance in magma genesis; regularities in the shift of the liquidus boundaries involving olivine, pyroxene, and silica minerals. Am. J. Sci. 275, 411–431.
Laubier, M., Grove, T.L., Langmuir, C.H., 2014. Trace element mineral/melt partitioning for basaltic and basaltic andesitic melts: an experimental and laser ICP-MS study with application to the oxidation state of mantle source regions. Earth Planet. Sci. Lett. 392, 265–278.
Le Roux, V., Dasgupta, R., Lee, C.T.A., 2011. Mineralogical heterogeneities in the earth's mantle: constraints from Mn, Co, Ni and Zn partitioning during partial melting. Earth Planet. Sci. Lett. 307, 395–408.
Lee, C.T.A., Leeman, W.P., Canil, D., Li, Z.X.A., 2005. Similar V/Sc systematics in MORB and arc basalts: Implications for the oxygen fugacities of their mantle source regions. J. Petrol. 46, 2313–2336.
Li, C.S., Ripley, E.M., 2010. The relative effects of composition and temperature on olivine-liquid Ni partitioning: statistical deconvolution and implications for petrologic modeling. Chem. Geol. 275, 99–104.
Li, C.S., Maier, W.D., De Waal, S.A., 2001. The role of magma mixing in the genesis of PGE mineralization in the Bushveld complex: Thermodynamic calculations and new interpretations. Econ. Geol. 96, 653–662.
Li, C.S., Thakurta, J., Ripley, E.M., 2012. Low-Ca contents and kink-banded textures are not unique to mantle olivine: evidence from the Duke Island complex, Alaska. Mineral. Petrol. 104, 147–153.
Li, C.S., Ripley, E.M., Thakurta, J., Stifter, E.C., Qi, L., 2013. Variations of olivine Fo-Ni contents and highly chalcophile element abundances in arc ultramafic cumulates, southern Alaska. Chem. Geol. 351, 15–28.
Liang, Z., 2018. Petrological and Geochemical Studies of Mafic-Ultramafic Complexes from Southeastern Alaska, United States. University of Chinese Academy of Sciences, Beijing.
Liu, X., Su, B.X., Bai, Y., Chen, C., Xiao, Y., Liang, Z., Yang, S.H., Peng, Q.S., Su, B.C., Liu, B., 2018. Ca-enrichment characteristics of parental magmas of chromitite in ophiolite: inference from mineral inclusions. Earth Sci. 43, 1038–1050 (In Chinese with English abstract).
Liu, X., Su, B.X., Xiao, Y., Chen, C., Uysal, I., Jing, J.J., Zhang, P.F., Chu, Y., Lin, W., Asamoah Sakyi, P., 2019. Initial subduction of Neo-Tethyan Ocean: geochemical records in chromite and mineral inclusions in the Pozantı-Karsantı ophiolite, southern Turkey. Ore Geol. Rev. 110, 102926.
Lynn, K.J., Shea, T., Garcia, M.O., Costa, F., Norman, M.D., 2018. Lithium diffusion in olivine records magmatic priming of explosive basaltic eruptions. Earth Planet. Sci. Lett. 500, 127–135.
Maier, W.D., Groves, D.I., 2011. Temporal and spatial controls on the formation of magmatic PGE and Ni-Cu deposits. Mineral. Deposita 46, 841–857.
Mallmann, G., O'Neill, H.S.C., 2009. The crystal/melt partitioning of V during mantle melting as a function of oxygen fugacity compared with some other elements (Al, P, Ca, Sc, Ti, Cr, Fe, Ga, Y, Zr and Nb). J. Petrol. 50, 1765–1794.
Mallmann, G., O'Neill, H.S.C., Klemme, S., 2009. Heterogeneous distribution of phosphorus in olivine from otherwise well-equilibrated spinel peridotite xenoliths and its implications for the mantle geochemistry of lithium. Contrib. Mineral. Petrol. 158, 485–504.
Matzen, A.K., Baker, M.B., Beckett, J.R., Stolper, E.M., 2013. The temperature and pressure dependence of nickel partitioning between olivine and silicate melt. J. Petrol. 54, 2521–2545.
Matzen, A.K., Baker, M.B., Beckett, J.R., Wood, B.J., Stolper, E.M., 2017. The effect of liquid composition on the partitioning of Ni between olivine and silicate melt. Contrib. Mineral. Petrol. 172, 3.
McDonough, W.F., Sun, S.S., 1995. The composition of the Earth. Chem. Geol. 120, 223–253.
Murray, G.C., 1972. Zoned ultramafic complexes of the Alaskan type: Feeder pipes of andesitic volcanoes. Geol. Soc. Am. 132, 313–335.
Nishimura, C.E., Forsyth, D.W., 1989. The anisotropic structure of the upper mantle in the Pacific. Geophys. J. Int. 96, 203–229.
Noble, J.A., 1960. Correlation of the ultramafic complexes of south eastern Alaska with those of other parts of North America and the world. Petrographic Provinces, Igneous Metamorphic Rocks. 21st International Geological Congress, Copenhagen, pp. 188–197.
Pagé, P., Barnes, S.J., 2009. Using trace elements in chromites to constrain the origin of podiform chromitites in the Thetford Mines ophiolite, Québec, Canada. Econ. Geol. 104, 997–1018.
Pearson, D.G., Canil, D., Shirey, S.B., 2003. Mantle samples included in volcanic rocks: xenoliths and diamonds. In: Carlson, R.W. (Ed.), Treatise on Geochemistry. 2. Elsevier, p. 568.
Prelević, D., Jacob, D.E., Foley, S.F., 2013. Recycling plus: a new recipe for the formation of Alpine-Himalayan orogenic mantle lithosphere. Earth Planet. Sci. Lett. 362, 187–197.
Ruckmick, J.C., Noble, J.A., 1959. Origin of the ultramafic complex at Union Bay, southeastern Alaska. Bull. Geol. Soc. Am. 70, 981–1017.

Rudnick, R.L., McDonough, W.F., Orpin, A., 1994. Northern Tanzanian peridotite xenoliths: a comparison with Kaapvaal peridotites and inferences on metasomatic interactions. In: Meyer, H., Leondaros, O. (Eds.), Kimberlites, Related Rocks and Mantle Xenoliths, Proceedings of the Fifth International Kimberlite Conference. Companhia de Pesquisa de Recursos Minerais, Brazil, Brasilia, pp. 336–353.

Sanfilippo, A., Tribuzio, R., Tiepolo, M., 2014. Mantle-crust interactions in the oceanic lithosphere: Constraints from minor and trace elements in olivine. Geochim. Cosmochim. Acta 141, 423–439.

Scoon, R.N., Klerk, W.J.D., 1987. The relationship of olivine cumulates and mineralization to cyclic units in part of the Upper critical zone of the western Bushveld complex. Can. Mineral. 25, 51–77.

Simkin, T., Smith, J.V., 1970. Minor-element distribution in olivine. J. Geol. 78, 304–325.

Sobolev, A.V., Hofmann, A.W., Sobolev, S.V., Nikogosian, I.K., 2005. An olivine-free mantle source of Hawaiian shield basalts. Nature 434, 590–597.

Sobolev, A.V., Hofmann, A.W., Kuzmin, D.V., Yaxley, G.M., Arndt, N.T., Chung, S.L., Danyushevsky, L.V., Elliott, T., Frey, F.A., Garcia, M.O., Gurenko, A.A., Kamenetsky, V.S., Kerr, A.C., Krivolutskaya, N.A., Matvienkov, V.V., Nikogosian, I.K., Rocholl, A., Sigurdsson, I.A., Sushchevskaya, N.M., Teklay, M., 2007. The amount of recycled crust in sources of mantle-derived melts. Science 316, 412–417.

Sobolev, N.V., Logvinova, A.M., Zedgenizov, D.A., Pokhilenko, N.P., Kuzmin, D.V., Sobolev, A., 2008. Olivine inclusions in Siberian diamonds: high-precision approach to minor elements. Eur. J. Mineral. 20, 305–315.

Sobolev, N.V., Logvinova, A.M., Zedgenizov, D.A., Pokhilenko, N.P., Malygina, E.V., Kuzmin, D.V., Sobolev, A.V., 2009. Petrogenetic significance of minor elements in olivines from diamonds and peridotite xenoliths from kimberlites of Yakutia. Lithos 112, 701–713.

Su, B.X., Gu, X.Y., Deloule, E., Zhang, H.F., Li, Q.L., Li, X.H., Vigier, N., Tang, Y.J., Tang, G.Q., Liu, Y., Pang, K.N., Brewer, A., Mao, Q., Ma, Y.G., 2015a. Potential orthopyroxene, clinopyroxene and olivine reference materials for in situ lithium isotope determination. Geostand. Geoanal. Res. 39, 357–369.

Su, B.X., Teng, F.Z., Hu, Y., Shi, R.D., Zhou, M.F., Zhu, B., Liu, F., Gong, X.H., Huang, Q.S., Xiao, Y., 2015b. Iron and magnesium isotope fractionation in oceanic lithosphere and sub-arc mantle: perspectives from ophiolites. Earth Planet. Sci. Lett. 430, 523–532.

Su, B.X., Chen, C., Pang, K.N., Sakyi, P.A., Uysal, I., Avci, E., Liu, X., Zhang, P.F., 2018. Melt penetration in oceanic lithosphere: Li isotope records from the Pozantı-Karsantı ophiolite in southern Turkey. J. Petrol. 59, 191–205.

Su, B., Chen, Y., Mao, Q., Zhang, D., Jia, L.H., Guo, S., 2019a. Minor elements in olivine inspect the petrogenesis of orogenic peridotites. Lithos 344-345, 207–216.

Su, B.X., Zhou, M.F., Jing, J.F., Robinson, P.T., Chen, C., Xiao, Y., Liu, X., Shi, R.D., Lenaz, D., Hu, Y., 2019b. Distinctive melt activity and chromite mineralization in Luobusa and Purang ophiolites, southern Tibet: constraints from trace element compositions of chromite and olivine. Sci. Bull. 64, 108–121.

Tang, Y.J., Zhang, H.F., Deloule, E., Su, B.X., Ying, J.F., Xiao, Y., Hu, Y., 2012. Slab-derived lithium isotopic signatures in mantle xenoliths from northeastern North China Craton. Lithos 149, 79–90.

Taylor, H.P.J., 1967. The zoned ultramafic complexes of southeastern Alaska, Part 4. In: Wiley, J. (Ed.), Ultramafic and Related Rocks, New York, pp. 96–118.

Thakurta, J., Ripley, E.M., Li, C., 2008. Geochemical constraints on the origin of sulfide mineralization in the Duke Island complex, southeastern Alaska. Geochem. Geophys. Geosyst. 9.

Wager, L.R., Brown, G.M., 1968. Layered Igneous Rocks. Oliver and Boyd, Edinburgh.

Wan, Z., Coogan, L.A., Canil, D., 2008. Experimental calibration of aluminum partitioning between olivine and spinel as a geothermometer. Am. Mineral. 93, 1142–1147.

Wang, J., Su, B.X., Tang, G.Q., Gao, B.Y., Wu, S.T., Li, J., 2020. Olivine, clinopyroxene and orthopyroxene reference materials for Li and O isotope in-situ microanalyses and their trace element compositions. Acta Petrol. Sinica 36, 1274–1284 (in Chinese with English abstract).

Winter, J.D., 2013. Principles of Igneous and Metamorphic Petrology. Pearson Education.

Xiao, Y., Teng, F.Z., Su, B.X., Hu, Y., Zhou, M.F., Zhu, B., Shi, R.D., Huang, Q.S., Gong, X.H., He, Y.S., 2016. Iron and magnesium isotopic constraints on the origin of chemical heterogeneity in podiform chromitite from the Luobusa ophiolite, Tibet. Geochem. Geophys. Geosyst. 17, 940–953.

Zanetti, A., Tiepolo, M., Oberti, R., Vannucci, R., 2004. Trace-element partitioning in olivine: Modelling of a complete data set from a synthetic hydrous basanite melt. Lithos 75, 39–54.